Magnetic moment force and semi-free electrons: a first-principles model for fast magnetic reconnection

Yuanjie Huang

Mianyang, Sichuan province, People's Republic of China

*Corresponding author's E-mail: hyj201207@163.com

Abstract

A long-standing puzzle in plasma physics is the universally fast rate of magnetic reconnection, observed to be of order 0.1 across diverse environments yet unexplained by classical resistive magnetohydrodynamics (MHD). We propose a new analytical model for two-dimensional steady-state reconnection based on two concepts: the magnetic moment force as the gyro-averaged Lorentz force, and the semi-free electron constraint arising from quasi-neutrality. We show that the inflow is driven by the magnetic moment force rather than resistive diffusion, while the outflow is governed by the ion pressure gradient. The model yields a closed-form reconnection rate that depends only on the electron-to-ion temperature ratio and ion charge state, independent of system size, field strength, density, and resistivity. For a thermal equilibrium hydrogen plasma, the rate is approximately 0.2, consistent with satellite observations and simulations. The model also reproduces the bipolar electrostatic field at the current sheet center. Compared with Sweet-Parker, Petschek, and Hall-MHD models, our framework offers a first-principles kinetic explanation for the universal reconnection rate. Finally, we propose a corresponding modification to the two-fluid MHD equations, removing the electron pressure gradient and replacing the Lorentz force with the magnetic moment force.

1. Introduction

Magnetic reconnection is a fundamental plasma process in which the topology of magnetic field lines is rearranged, leading to the explosive conversion of stored magnetic energy into plasma kinetic and thermal energy [1, 2]. This process drives some of the most energetic phenomena in the universe, including solar flares, coronal mass ejections, magnetospheric substorms, and astrophysical jets [3, 4]. Understanding magnetic reconnection is therefore not only a cornerstone of plasma physics but also essential for explaining and predicting space weather and high-energy astrophysical events.

Despite decades of research, the anomalously fast reconnection rate remains a central puzzle. Early theoretical models, such as the Sweet-Parker model [5, 6, 7], described reconnection within resistive magnetohydrodynamics (MHD) and predicted a rate far too slow to explain the rapid energy release observed in solar flares and the Earth's magnetosphere [7]. This model's slow rate stems from a mass-conservation bottleneck, where all inflowing plasma must be expelled through a narrow, resistive diffusion region. The Petschek model attempted to resolve this by invoking slow shocks to broaden the outflow region [8], but it was found to be unstable and inapplicable for systems with uniform resistivity [9, 10].

The advent of in-situ observations from missions like Cluster and, more recently, the Magnetospheric Multiscale (MMS) mission has provided direct evidence that reconnection in space plasmas proceeds at a normalized rate of approximately 0.1, independent of the specific dissipation mechanism [3, 11, 12]. This has prompted a paradigm shift from collision-dominated MHD models to collisionless kinetic theories. The inclusion of the Hall term in the generalized Ohm's law, representing the decoupling of ion and electron motions, has been shown to be critical for enabling fast reconnection [11, 13]. The Hall effect generates a quadrupolar out-of-plane magnetic field and a diverging Poynting flux that “diverts” electromagnetic energy away from the X-line, which appears to be key to localizing the diffusion region and achieving a fast rate [14].

However, a complete first-principles explanation for why the reconnection rate is universally of the order of 0.1 has remained elusive [12, 15]. Recent theoretical work suggests that the reconnection rate is not solely controlled by the microphysics of the electron diffusion region but is instead constrained by a global force balance in the upstream region [12, 14]. This “outside-in” approach proposes that the maximum possible reconnection rate is limited by the requirement to bend the upstream magnetic field lines into the diffusion region, leading to a maximum of ~0.2. Complementary to this macroscopic perspective, recent advancements in observational capabilities, particularly the Magnetospheric Multiscale (MMS) mission, have provided unprecedented access to the electron-scale physics that governs the diffusion region [16, 17]. These observations have revealed complex kinetic dynamics, including electron-only reconnection and the critical role of non-gyrotropic electron pressure tensors in balancing the reconnection electric field, thereby validating key predictions of kinetic theory [16, 17]. Despite these significant breakthroughs, the coupling between localized microphysics and the global system remains poorly understood. Key unresolved issues include the transition from electron-only to ion-coupled reconnection, the dynamical evolution of X-lines, and the mechanisms governing energy partition and the onset of explosive events [18]. Addressing these cross-scale coupling problems requires a theoretical framework that can bridge the gap between the kinetic-scale processes in the diffusion region and the macroscopic constraints imposed by the surrounding plasma.

In this paper, we build upon these recent insights by developing a new analytical model for two-dimensional magnetic reconnection. Our model focuses on the anisotropic pressure and flow dynamics within the diffusion region and provides a self-consistent expression for the reconnection rate. We demonstrate that this rate is fundamentally dependent on the electron-to-ion temperature ratio, thereby providing a direct link between kinetic-scale physics and global reconnection dynamics.

2. Theoretical methods

2.1 Magnetic moment force: gyro-averaged description of Lorentz force

The concept of the magnetic moment force, as a gyro-averaged alternative to the Lorentz force, was previously applied to anomalous transport in tokamak plasmas [19]. This concept is briefly reviewed below.

A charged particle in a magnetic field experiences the Lorentz force and typically follows a helical trajectory. According to conventional transport theory, the Lorentz force does no work, as it remains perpendicular to the particle velocity.

On time and spatial scales much larger than the gyroperiod and gyroradius, the particle motion can be described in terms of its guiding center. Over a complete gyroperiod, the guiding center experiences a net drift force. Under the condition $|r_{c\alpha}\nabla B_z/B_z| \ll 1$, this drift force reduces to the magnetic moment force [19, 20],

$$\vec{F}_{\alpha m} = -\frac{m_\alpha v_{\alpha\perp}^2}{2B_z}\nabla_\perp B_z \tag{1}$$

where the species subscript $\alpha = i, e$ denotes ions and electrons, $r_{c\alpha}$ is the gyration radius, $F_{\alpha m}$ the magnetic moment force for the species α, $v_{\alpha\perp}$ the particle velocity perpendicular to the magnetic field, and B_z the magnetic field strength along the z direction.

Replacing the Lorentz force with this magnetic moment force reveals the underlying physics of the magnetic reconnection rate.

2.2 Semi-free electrons in neutral plasma

The concept of semi-free electrons was introduced to explain plasma thermal conductivity and anomalous transport in tokamak plasmas [19, 21]. We briefly summarize it here.

In a steady-state quasi-neutral plasma, owing to charge neutrality, the positions of ions and electrons cannot be distinguished within an infinitesimal volume element in the sense of calculus. Moreover, the momentum of such a plasma element is dominated by ions due to their much larger masses. Consequently, the ionized electrons do not possess independent positional degrees of freedom and their positions are determined by the ions in the same plasma element through the strong electrostatic force. This situation is analogous to that of neutral gases, in which light electrons are bound to heavy nuclei and thus lack positional degrees of freedom. Therefore, the ionized electrons in a quasi-neutral plasma are more appropriately described as semi-free electrons. This concept constitutes a crucial physical insight for understanding transport phenomena in quasi-neutral plasmas. Accordingly, the physical constraint in mathematics is given by

$$\nabla f_e = 0 \tag{2}$$

where f_e is the distribution function for semi-free electrons. This treatment deviates substantially from conventional theoretical approaches and, as shown later, determines the sign of the electrostatic field in magnetic reconnection.

3. Results and Discussion

3.1 Magnetic reconnection rate

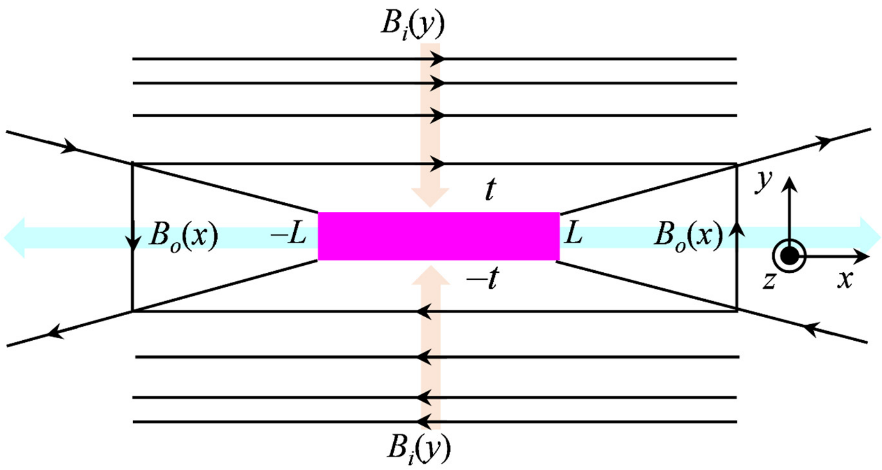

Figure 1 Schematic diagram for the two-dimensional magnetic reconnection. The coordinates are shown by the inset. The black arrows denote the direction of the magnetic fields $B_i(y)$, $B_o(x)$. The magenta region signifies the electric current sheet with the width $2L$ and thickness $2t$.

The schematic diagram for the two-dimensional magnetic reconnection is shown in Fig. 1.

The current density along z direction in the current sheet is

$$j_z(x,y)=\sigma_e v_i B_{ix}(y)=\sigma_e v_o B_{oy}(x)=j_z$$

where v_i and v_o denote the inflow and outflow velocities, respectively. The current density is treated as a constant in the first-order approximation. $B_i(y)$ and $B_o(x)$ are the position-dependent magnetic fields close to the inflow and outflow sides of the electric current sheet (ECS), oriented along the x- and y-directions, respectively. Based on Maxwell equations, it satisfies the following relation

$$\frac{\partial B_i(y)}{\partial y}=-\mu_0\sigma_e v_i B_i(y) \tag{3}$$

Along x direction, the magnetic field $B_o(x)$ can be given by

$$B_o(x)=\frac{\mu_0}{4\pi}\iiint\frac{(x-x')j_z}{\left[(x-x')^2+y^2+z^2\right]^{3/2}}=\frac{\mu_0 j_z}{2\pi}\iint\frac{(x-x')}{(x-x')^2+y^2}=\frac{\mu_0}{2\pi}\frac{1}{2}\int_{-t}^{t}dy\ln\frac{4x^2+y^2}{y^2}$$

$$=\frac{\mu_0 j_z}{4\pi}\left[4x\pi-8xArc\tan\left(\frac{2x}{t}\right)+2t\ln\left(1+\frac{4x^2}{t^2}\right)\right]$$

$$=\frac{\mu_0 j_z}{\pi}x\left[\pi-2Arc\tan\left(\frac{2x}{t}\right)+\frac{t}{2x}\ln\left(1+\frac{4x^2}{t^2}\right)\right]\approx\frac{\mu_0 j_z t}{\pi}\left[1+\ln\frac{2x}{t}\right]$$

It is

$$B_o(x)\approx\frac{\mu_0 j_z t}{\pi}\left[1+\ln\frac{2x}{t}\right]$$

Therefore, the outflow velocity at position (L, 0) can be obtained

$$v_o\approx\frac{\pi}{\mu_0\sigma_e t\left[1+\ln\frac{2L}{t}\right]} \tag{4}$$

The spatial gradient of the magnetic field $B_o(x)$ along x direction follows that

$$\frac{\partial\ln B_o(x)}{\partial x}\approx\frac{\mu_0\sigma_e v_o}{\pi}\frac{t}{x} \tag{5}$$

Assuming Maxwellian distributions for the ions and electrons, the related anisotropic components are

$$f_e^1=\frac{\tau_e f_e^0\vec{v}_e\cdot}{k_B T_e}\left[e\vec{E}_x+e\vec{E}_y-\frac{m_e v_{e\perp}^2}{2B_i(y)}\frac{\partial}{\partial y}B_i(y)\vec{e}_y-\frac{m_e v_{e\perp}^2}{2B_o(x)}\frac{\partial}{\partial x}B_o(x)\vec{e}_x+eE_z\vec{e}_z\right]$$

$$f_i^1 = \frac{\tau_i f_i^0 \vec{v}_i \cdot}{k_B T_i}\left[-k_B T_i \nabla \ln p_i(r) - k_B T_i\left(\frac{v_i^2}{v_{iT}^2}-\frac{5}{2}\right)\nabla \ln T_i - Ze\vec{E}_x - Ze\vec{E}_y - \frac{m_i v_{i\perp}^2}{2B_i(y)}\frac{\partial}{\partial y}B_i(y)\vec{e}_y - \frac{m_i v_{i\perp}^2}{2B_o(x)}\frac{\partial}{\partial x}B_o(x)\vec{e}_x - ZeE_z\vec{e}_z\right]$$

where τ_e, τ_i signify the electron and ion relaxation times, respectively, E_x, E_y, E_z represent the electric field in x, y, z directions, $p_i(r)$ is the position-dependent ion pressure, $v_{e\perp}$, $v_{i\perp}$ stand for the electron and ion velocities perpendicular to the magnetic field, $v_{\alpha T} = \sqrt{2k_B T_\alpha / m_\alpha}$ is the thermal speed of species α, and temperatures T_α may be position-dependent, α=i, e for ions and electrons, $\vec{e}_x$, $\vec{e}_y$,$\vec{e}_z$ denote the unit direction vectors.

The inflow and outflow velocities of the electrons and ions can be derived as

$$v_{e-i} = \frac{\tau_e}{m_e}\left[e\vec{E}_y - \frac{5k_B T_e}{3B_i(y)}\frac{\partial}{\partial y}B_i(y)\vec{e}_y\right]$$

$$v_{e-o} = \frac{\tau_e}{m_e}\left[e\vec{E}_x - \frac{5k_B T_e}{3B_o(x)}\frac{\partial}{\partial x}B_o(x)\vec{e}_x\right]$$

$$v_{i-i} = \frac{\tau_i}{m_i}\left[-k_B T_i\frac{\partial}{\partial y}\ln p_i(r) - Ze\vec{E}_y - \frac{5k_B T_i}{3B_i(y)}\frac{\partial}{\partial y}B_i(y)\vec{e}_y\right]$$

$$v_{i-o} = \frac{\tau_i}{m_i}\left[-k_B T_i\frac{\partial}{\partial x}\ln p_i(r) - Ze\vec{E}_x - \frac{5k_B T_i}{3B_o(x)}\frac{\partial}{\partial x}B_o(x)\vec{e}_x\right]$$

where Z denotes the charge state of ion.

Charge neutrality requires identical electron and ion velocities. Thus, the inflow velocity can be formulated

$$\left(\frac{\tau_e}{m_e}+\frac{Z\tau_i}{m_i}\right)v_i = -\frac{\tau_e}{m_e}\frac{\tau_i}{m_i}k_B T_i\frac{\partial}{\partial y}\ln p_i(r) - \frac{\tau_i}{m_i}\frac{\tau_e}{m_e}\frac{5k_B(ZT_e+T_i)}{3B_i(y)}\frac{\partial}{\partial y}B_i(y)$$

Using Eq. (3), the inflow velocity can be obtained

$$v_i = -\frac{\frac{\tau_e}{m_e}\frac{\tau_i}{m_i}\left(\frac{\tau_e}{m_e}+\frac{Z\tau_i}{m_i}\right)^{-1}k_B T_i\frac{\partial}{\partial y}\ln p_i(r)}{1-\frac{\tau_i}{m_i}\frac{\tau_e}{m_e}\left(\frac{\tau_e}{m_e}+\frac{Z\tau_i}{m_i}\right)^{-1}\frac{5k_B(ZT_e+T_i)}{3}\mu_0\sigma_e} \approx \frac{3}{5}\frac{T_i}{(ZT_e+T_i)}\frac{1}{\mu_0\sigma_e}\frac{\partial}{\partial y}\ln p_i(r) \qquad (6)$$

The pressure and magnetic field satisfy the relation

$$0 \approx \frac{\partial}{\partial y}\left[\ln p_i(r) B_i(y)^{5(ZT_e+T_i)/3T_i}\right] \tag{7}$$

$$\frac{\partial}{\partial y}\ln B_i(y) \approx -\frac{3T_i}{5(ZT_e+T_i)}\frac{\partial}{\partial y}\ln p_i(r)$$

Therefore, the inflow velocity is formulated as

$$v_i \approx -\frac{1}{\mu_0\sigma_e}\frac{\partial}{\partial y}\ln B_i(y) \tag{8}$$

Furthermore, the reconnection electric field along z direction can be given by

$$E_z \approx \frac{1}{\mu_0\sigma_e}\frac{\partial}{\partial y}B_i(y) \tag{9}$$

Thus, the steady-state reconnection electric field is proportional to the spatial gradient of $B_i(y)$, not its magnitude. Consequently, the reconnection electric field at the null point is much larger than predicted by conventional theory.

The related electrostatic field in y direction is given by

$$e\vec{E}_y = \left(\frac{3}{5}\frac{1}{\frac{\tau_e}{m_e}}\frac{1}{\mu_0\sigma_e} - k_B T_e\right)\frac{T_i}{(ZT_e+T_i)}\frac{\partial}{\partial y}\ln p_i(r) \approx -\frac{k_B T_e}{(ZT_e/T_i+1)}\frac{\partial}{\partial y}\ln p_i(r) \tag{10}$$

$$e\vec{E}_y \approx \frac{5k_B T_e}{3}\frac{\partial}{\partial y}\ln B_i(y)$$

Taking the assumption

$$-\frac{\partial}{\partial y}\ln p_i(r) \approx \frac{1}{t}$$

The electric field along y direction can be given by

$$e\vec{E}_y \approx \frac{T_i}{(ZT_e+T_i)}\frac{k_B T_e}{t}$$

It follows that the normal electric field points towards the ECS center and reverses at the center. This agrees with the experimental results that the normal component of the electric field has a bipolar signature and the reversal happens at the center of ECS [2]. The negative electric field here and in tokamak plasmas verifies the validity of semi-free electrons. The magnitude of E_y scales with $-\nabla p_i(r)/en_i$, consistent with the simulations [2]. For a plasma with the electron temperature 1 KeV and the ECS thickness 10^5 m at the top of the Earth's magnetosphere [2, 3, 22], the electric field reaches the order of 10 mV/m, in agreement with the experimental observations [2, 3, 22]. These results show that the magnetic moment force, rather than the pressure gradient or the electrostatic force, drives the inflow and generates the ion pressure gradient, which in turn drives the outflow.

Similarly, the outflow velocity can be obtained

$$\left(\frac{\tau_e}{m_e}+\frac{Z\tau_i}{m_i}\right)v_o=-\frac{\tau_e}{m_e}\frac{\tau_i}{m_i}k_BT_i\frac{\partial}{\partial x}\ln p_i(r)-\frac{\tau_e}{m_e}\frac{\tau_i}{m_i}\frac{5k_B(ZT_e+T_i)}{3B_o(r)}\frac{\partial}{\partial x}B_o(x)$$

The relation between the ion pressure and the magnetic field can be approximated as

$$0\approx\frac{\partial}{\partial x}\left[\ln p_i(r)B_o(x)^{5(ZT_e+T_i)/3T_i}\right]$$

$$\frac{3T_i}{5(ZT_e+T_i)}\frac{\partial}{\partial x}\ln p_i(r)=-\frac{\partial}{\partial x}\ln B_o(x) \tag{11}$$

Considering Eq. (5), the outflow velocity is given by

$$v_{i-o}=\frac{-\frac{\tau_e}{m_e}\frac{\tau_i}{m_i}\left(\frac{\tau_e}{m_e}+\frac{Z\tau_i}{m_i}\right)^{-1}k_BT_i\frac{\partial}{\partial x}\ln p_i(r)}{\left[1+\frac{\tau_e}{m_e}\frac{\tau_i}{m_i}\left(\frac{\tau_e}{m_e}+\frac{Z\tau_i}{m_i}\right)^{-1}\frac{5k_B(ZT_e+T_i)}{3}\frac{\mu_0\sigma_e}{\pi}\frac{t}{x}\right]}\approx\frac{-k_BT_i\frac{\partial}{\partial x}\ln p_i(r)}{\frac{5k_B(ZT_e+T_i)}{3}\frac{\mu_0\sigma_e}{\pi}\frac{t}{x}}=-\frac{3}{5}\frac{T_i}{(ZT_e+T_i)}\frac{\pi}{\mu_0\sigma_e}\frac{x}{t}\frac{\partial}{\partial x}\ln p_i(r)$$

The electric field follows as

$$e\vec{E}_x=\frac{v_o}{\frac{\tau_e}{m_e}}+\frac{5k_BT_e}{3B_o(x)}\frac{\partial}{\partial x}B_o(x)\vec{e}_x=\frac{v_o}{\frac{\tau_e}{m_e}}+\frac{5k_BT_e}{3B_o(x)}\frac{\mu_0 j_z}{\pi}\frac{t}{x}=\frac{v_o}{\frac{\tau_e}{m_e}}+\frac{5k_BT_e}{3}\frac{\mu_0\sigma_e}{\pi}\frac{t}{x}v_o\approx\frac{5k_BT_e}{3}\frac{\mu_0\sigma_e}{\pi}\frac{t}{x}v_o$$
$$=\frac{5k_BT_e}{3}\frac{\mu_0\sigma_e}{\pi}\frac{t}{x}\left[-\frac{3}{5}\frac{T_i}{(ZT_e+T_i)}\frac{\pi}{\mu_0\sigma_e}\frac{x}{t}\frac{\partial}{\partial x}\ln p_i(r)\right]$$
$$=-\frac{k_BT_e}{(ZT_e/T_i+1)}\frac{\partial}{\partial x}\ln p_i(r)$$

Using Eq. (11), the electric field can be written as

$$e\vec{E}_x\approx\frac{5k_BT_e}{3}\frac{\partial}{\partial x}\ln B_o(x) \tag{12}$$

Similarly, E_x also points to the ECS center with a reversal at the center. The ratio of the magnitude of the electric fields is given by

$$\frac{E_x}{E_y}=\frac{\frac{\partial}{\partial x}\ln p_i\left(r\right)}{\frac{\partial}{\partial y}\ln p_i\left(r\right)}\sim\frac{t}{L}=R_{mr}$$

where R_{mr} signifies the magnetic reconnection rate (MRR). Combining Eq. (4) and Eq. (6) yields

$$R_{mr}=\frac{v_i}{v_o}\approx\frac{\frac{3}{5}\frac{T_i}{\left(ZT_e+T_i\right)}\frac{1}{\mu_0\sigma_e}\frac{\partial}{\partial y}\ln p_i\left(r\right)}{\frac{\pi}{\mu_0\sigma_e t\left[1+\ln\frac{2L}{t}\right]}}\approx\frac{3}{5\pi}\frac{T_i}{\left(ZT_e+T_i\right)}\left[1+\ln\frac{2L}{t}\right]$$

which satisfies the following relation

$$R_{mr}-\frac{3}{5\pi}\frac{T_i}{\left(ZT_e+T_i\right)}\left[1+\ln 2-\ln R_{mr}\right]=0$$

The solution is then given by

$$R_{mr}=\frac{3}{5\pi}\frac{T_i}{\left(ZT_e+T_i\right)}W\left[\frac{10\pi exp(1)}{3}\frac{\left(ZT_e+T_i\right)}{T_i}\right] \tag{13}$$

where W is the Lambert W-function, defined by $W[x\cdot exp(x)]=x$.

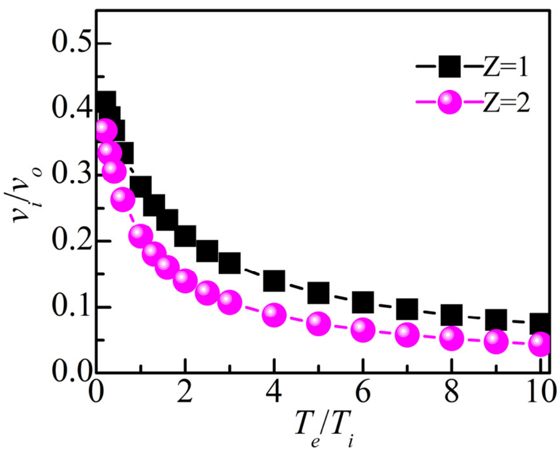

Figure 2 The magnetic reconnection rate versus the temperature-dependent parameter T_e/T_i. T_i, T_e denote the ion temperature and electron temperature, respectively, Z signifies the net charge nucleus of the ion.

The rate is independent of spatial scales, magnetic field strength, plasma density and electric conductivity. This is consistent with the conclusions that the MRR does not depend on the thickness of current sheet [17] and the reconnection rate is insensitive to the dissipation mechanism in Geospace Environmental Modeling (GEM) [2, 11]. It also agrees with observations that the MRR is of order 0.1 across diverse systems [4, 15] and it is mostly independent of the system parameters [4]. The MRR depends only on Z and the ratio T_e/T_i. Eq. (13) yields two predictions. (i) The MRR decreases with increasing T_e/T_i, and (ii) the MRR decreases with increasing Z.

For a hydrogen-helium mixture (Z=1, 2) in the thermal equilibrium (T_e=T_i), the MRR is ~0.2, much higher than the conventional Sweet-Parker model but consistent with the observations and simulations that the steady-state MRR is of the order of 0.1 [4, 12, 15, 16, 17]. The POLAR satellite measurement gave the results [2, 23] $|E_z|\approx 5$mV/m, $|E_x|\approx 25$mV/m, which yield the MRR $R_{mr}\approx 0.2$.

Using Eq. (4) and the definition of MRR, the reconnection time scale can be given by [16]

$$\tau_{rec} \sim \frac{L}{v_i} = \frac{\mu_0 \sigma_e L^2}{\pi}\left[1+\ln\left(2/R_{mr}\right)\right] \tag{14}$$

where τ_{rec} signifies the magnetic reconnection time scale. The relation may be utilized to estimate the electric conductivity.

3.2 Energy conversion

The rate of inflow of electromagnetic energy can be given by the Poynting flux $v_i B_i^2 L/\mu_0$.The ratio of the inflow kinetic energy to the electromagnetic energy is given by

$$\frac{1}{2}\frac{\rho v_i^2}{B_i^2/\mu_0}=\frac{v_i^2}{2v_{Ai}^2}$$

where v_{Ai} denotes Alfvén speed. And the ratio of the outflow kinetic energy to the electromagnetic energy is

$$\frac{1}{2}\frac{\rho v_o^2 v_o t}{v_i L B_i^2/\mu_0}=\frac{1}{R_{mr}^2}\frac{v_i^2}{2v_{Ai}^2} \tag{15}$$

Thus, the energy conversion efficiency is inversely proportional to the square of the MRR. A smaller MRR yields larger energy conversion. Since a larger T_e/T_i corresponds to a smaller MRR, it also yields more efficient energy conversion.

3.3 Comparison with mainstream models

The central unresolved problem in magnetic reconnection research has been the theoretical explanation of the fast, universal reconnection rate of order 0.1, a value that is robustly observed in space, solar, and laboratory plasmas [2, 12]. The analytical model presented in this work offers a novel, first-principles derivation of this rate, which contrasts sharply with the existing paradigms reviewed in the literature. A detailed comparison with the dominant theoretical models, namely, the Sweet-Parker model, the Petschek model, and the two-fluid/Hall MHD model is essential for contextualizing the contributions of this new theory.

3.3.1. The Sweet-Parker Model and the Scaling Problem

The Sweet-Parker model as reviewed [2] is the foundational resistive MHD description of reconnection. It posits a diffusion region of length $2L$ and width $2t$, where plasma is ejected at the Alfvén speed. This leads to a reconnection rate R_{mr}~$S^{-1/2}$, where S is the Lundquist number. For typical astrophysical and space plasmas with

$S \gg 1$, this rate is far too slow (e.g., $\sim 10^{-6}$ in the solar corona) to explain explosive energy release. The model's bottleneck arises from the requirement that all mass and flux pass through the narrow, resistive layer.

Our model departs fundamentally from the Sweet-Parker framework in two key aspects. First, the reconnection rate derived in Eq. (13) of our manuscript, is independent of the Lundquist number S and thus of the system's global scale and resistivity. This directly addresses the primary failure of the Sweet-Parker model, which is its strong dependence on S and its consequent inability to predict a rate of ~ 0.1 for realistic parameters. Second, our model identifies the primary driver of the inflow as the magnetic moment force, a gyro-averaged form of the Lorentz force, rather than the pressure gradients and resistive diffusion central to the Sweet-Parker description. This shift in the fundamental force balance allows the model to circumvent the mass-conservation bottleneck, as the inflow is no longer dictated by resistive diffusion but by a kinetic-scale force acting on the ionized species. The generalized Sweet-Parker model discussed [2] successfully describes reconnection in collisional regimes by incorporating compressibility and downstream pressure effects. However, it still operates within a resistive MHD framework and retains a dependence on an effective Lundquist number, making it inadequate for explaining the fast, universal rate observed in collisionless plasmas. Our model eliminates this dependence by identifying a fundamentally different kinetic-scale driver for the inflow.

3.3.2. The Petschek model and the role of slow shocks

The Petschek model was proposed to overcome the Sweet-Parker limitation by invoking slow shocks that emerge from a small central diffusion region, broadening the outflow channel and increasing the reconnection rate to R_{mr}~$\pi/8\ln(S)$ [2]. However, this model has been heavily debated. Biskamp [9] and later Uzdensky et.al [24] showed that for a constant resistivity, the Petschek solution is not self-consistent. Malyshkin et.al [10] further demonstrated that the Petschek configuration cannot satisfy the constraint imposed by the second derivative of Ohm's law at the X-point, thereby ruling out the existence of steady-state slow shocks for a uniform resistivity. The model's validity is generally restricted to cases with localized, strongly enhanced resistivity.

Our model does not invoke slow shocks or any other form of MHD discontinuities. The outflow is driven by the pressure gradient, which is a direct consequence of the ion pressure build-up, and the rate itself is determined entirely by local kinetic parameters (the electron-to-ion temperature ratio T_e/T_i and ion charge state Z). Although the Petschek model predicts a rate of order 0.1 via a weak logarithmic dependence on the global Lundquist number (R_{mr}~$\pi/8\ln S$), its underlying mechanism relies on slow shocks, which have been shown to be unsustainable for uniform resistivity. In contrast, our model derives a scale-invariant rate from purely local kinetic parameters without invoking such shocks. Our result that the rate is of order 0.1 for a thermal equilibrium hydrogen plasma (T_e/T_i=1, Z=1) aligns with the Petschek model's predictions for high-S systems, but our model achieves this without the contested shock structure and with a self-consistent kinetic foundation. Furthermore, the experimentally observed "double-wedge" profile in the collisionless MRX, cited by Yamada et al. [2], is often likened to

Petschek-like morphology, but our model suggests this profile is a manifestation of kinetic-scale pressure and force balance, not of slow shocks.

3.3.3. Two-Fluid and Hall MHD Models

The modern paradigm for fast reconnection, as extensively reviewed [2], centers on the Hall effects. When the ion skin depth exceeds the Sweet-Parker layer width, the decoupling of ion and electron motions becomes critical. The Hall term in the generalized Ohm's law generates a quadrupolar out-of-plane magnetic field and a fast reconnection electric field, leading to a rate that is insensitive to the specific dissipation mechanism and is on the order of 0.1. This was a key conclusion of the Geospace Environmental Modeling (GEM) challenge [11]. In the two-fluid picture, ions are demagnetized in the broader ion diffusion region, while electrons remain magnetized and flow in a thinner layer, enabling a fast reconnection rate that is independent of the microscopic resistivity [13].

Our model provides a complementary but distinct physical mechanism for the same observed phenomena. The Hall-MHD models attribute the fast rate to the Lorentz force acting differently on ions and electrons, with the Hall term directly supporting the reconnection electric field. Our model, in contrast, replaces the Lorentz force with the magnetic moment force for the guiding-center motion and introduces the concept of semi-free electrons. This concept, encapsulated in Eq. (2), posits that the electrons' positional degrees of freedom are constrained by charge neutrality, fundamentally altering the structure of the pressure tensor and the resulting electrostatic fields. The Hall-MHD models predict a reconnection rate that depends on the system size L and the ion skin depth d_i, often as $R_{mr} \sim d_i/L$ in the simplest scaling, though more refined theories suggest a universal constant of~0.1 [12, 14]. Our model derives a rate that is strictly a function of local temperature and charge parameters, providing a more fundamental constraint that is independent of spatial scales.

Crucially, our model reproduces the key experimental signatures of collisionless reconnection. The predicted quadrupolar out-of-plane field follows from the electron flow patterns, and the electric field profiles in the y and x directions are shown to agree with the bipolar normal electric field and the reconnection electric field measured in the MRX and by the CLUSTER and POLAR satellites, as discussed [2] and [23]. The derivation of the normal electric field E_y as a bipolar structure with a reversal at the center of the current sheet is a direct prediction of our semi-free electron model, and it is in quantitative agreement with the Cluster observations of a strong potential well [22]. This agreement suggests that the magnetic moment force and the semi-free electron constraint provide a more fundamental, first-principles description of the kinetic physics that the Hall-MHD models capture phenomenologically.

3.3.4. Global Constraints and the "Outside-In" Approach

A more recent theoretical development, often termed the 'outside-in' or global force-balance approach [12, 14], proposes that the reconnection rate is constrained by the global requirement to bend the upstream magnetic field. This perspective builds upon earlier studies on the effects of boundary conditions, such as those reviewed [2]. This model proposes that the reconnection rate is not solely determined by local microphysics in the electron diffusion region but is constrained by the global requirement to bend the upstream magnetic field lines into the diffusion region. This yields a maximum local reconnection rate of approximately 0.1~0.2, which is independent of the microscopic dissipation.

Our model aligns remarkably well with this global perspective. While our derivation is based on local kinetic-scale physics (the magnetic moment force and semi-free electrons), the resulting reconnection rate is a constant determined by fundamental plasma parameters, making it naturally independent of global system size and boundary conditions. The rate of ~0.2 for T_e/T_i=1 and Z=1 in Eq. (13) matches the predicted upper limit of the outside-in model. However, our model goes further by providing a mechanism for why this limit is set: the ratio T_e/T_i fundamentally governs the ion pressure gradient and the electrostatic field structure, which in turn determine the maximum inflow and outflow speeds. In this sense, our model bridges the local kinetic physics and the global constraint by showing that the maximum rate is a thermodynamic property of the plasma, not just a consequence of geometry.

3.3.5. Summary of the Comparison

Table 1 summarizes the key differences between our model and the established theories.

Table 1 the differences between the theories and our model for the magnetic reconnection rate.

Feature	Sweet-Parker (MHD)	Petschek	Hall MHD / Two-Fluid	This Work
Underlying Physics	Resistive MHD, mass conservation	Resistive MHD + slow shocks	Hall term in Ohm's law, ion-	Magnetic moment force,

			electron decoupling	semi-free electrons
Rate Dependence	$R_{mr} \sim S^{-1/2}$ (strongly scale-dependent)	$R_{mr} \sim \pi/(8\ln S)$ (weakly scale-dependent)	$R_{mr} \sim 0.1$ (universal, independent of resistivity)	$R_{mr} = f(T_e/T_i, Z)$ (universal, scale-independent)
Primary Driver of Inflow	Resistive diffusion	Resistive diffusion	Hall electric field	Magnetic moment force
Role of Shocks	None	Central to the model	None	None
Scale of Rate	Dependent on global length L	Dependent on L through $\ln S$	Constrained by global upstream field, but local rate is universal	Determined solely by local kinetic parameters

Our analytical model provides a novel and self-consistent derivation of the fast reconnection rate that is independent of system scale and resistivity, resolving the central puzzle of the Sweet-Parker model. It offers a complementary kinetic explanation to the Hall-MHD framework by identifying the magnetic moment force and the semi-free electron constraint as the fundamental mechanisms. The model's predictions for the rate's dependence on T_e/T_i and Z, and its agreement with observed electric field structures, suggest that it captures essential physics underlying the universal reconnection rate across diverse plasma environments. This work potentially represents a significant step toward a unified theory by linking local kinetic thermodynamics to the global reconnection dynamics.

3.4 Modification of magnetohydrodynamics (MHD)

The analytical results presented above, together with the theoretical framework for plasma thermal transport [21] and anomalous transport in tokamak plasmas [19][19] , motivate a fundamental revision of the standard two-fluid MHD equations. Specifically, the conventional electron pressure gradient term ∇p_e should be omitted, and the Lorentz force should be replaced by the magnetic moment force in the momentum equations for both species.

In the conventional two-fluid MHD formulation [25, 26], the electron and ion momentum equations are written as:

$$n_e m_e \left[\frac{\partial \vec{u}_e}{\partial t} + \left(\vec{u}_e \cdot \nabla \right) \vec{u}_e \right] = n_e e \left(\vec{E} + \vec{u}_e \times \vec{B} \right) - \nabla p_e \tag{16}$$

$$n_i m_i \left[\frac{\partial \vec{u}_i}{\partial t} + \left(\vec{u}_i \cdot \nabla \right) \vec{u}_i \right] = -n_i Z e \left(\vec{E} + \vec{u}_e \times \vec{B} \right) - \nabla p_i \tag{17}$$

where $\vec{u}_e$ and $\vec{u}_i$ are the electron and ion fluid velocities, p_i, p_e signifies the ion pressure and electron pressure, and the remaining symbols follow their standard meanings.

Our analysis, however, indicates that ∇p_e does not represent a genuine force in a quasi-neutral plasma. This conclusion arises directly from the semi-free electron constraint in Eq. (2): the electron distribution function f_e is not an independent dynamical variable, and consequently, the electron pressure cannot support a macroscopic force. Physically, electrons lack independent positional degrees of freedom and their spatial distribution is dictated by ions through the strong electrostatic force required to maintain charge neutrality. Therefore, the term ∇p_e should be eliminated from the electron momentum equation.

Furthermore, on time and spatial scales much larger than the gyroperiod and gyroradius, the Lorentz force reduces to the magnetic moment force after gyro-averaging [19, 20]. This gyro-averaged force, given by Eq. (1), is the physically relevant force for the guiding-center motion of both species. Consequently, we replace the Lorentz force terms with their gyro-averaged counterparts, the magnetic moment forces for electrons and ions, respectively.

Applying these two modifications, the revised two-fluid momentum equations become

$$n_e m_e \left[\frac{\partial \vec{u}_e}{\partial t} + \left(\vec{u}_e \cdot \nabla \right) \vec{u}_e \right] = n_e e \vec{E} + \vec{F}_{em} \tag{18}$$

$$n_i m_i \left[\frac{\partial \vec{u}_i}{\partial t} + \left(\vec{u}_i \cdot \nabla \right) \vec{u}_i \right] = -n_i Z e \vec{E} + \vec{F}_{im} - \nabla p_i \tag{19}$$

where $\vec{F}_{im}$ and $\vec{F}_{em}$ are the magnetic moment forces for electrons and ions, as defined in Eq. (1).

In a thermal equilibrium plasma where T_e=T_i, the magnetic moment forces for electrons and ions satisfy $\vec{F}_{im} = \vec{F}_{em}$, reflecting the equipartition of energy between the two species. In more general cases, the two forces differ according to the respective temperatures.

The standard one-fluid MHD formulation is insufficient to capture the electrostatic field structure essential for reconnection physics. This limitation arises because the single-fluid model implicitly assumes equal ion and electron velocities and neglects the charge separation effects that give rise to the bipolar electric fields observed in the reconnection layer. The two-fluid formulation presented here, on the other hand, explicitly retains the distinct dynamics of electrons and ions and is therefore capable of describing the electrostatic potential structures such as the bipolar normal electric field given by Eq. (10).

In cases where the magnetic field has two perpendicular components, say B_y and B_z, the total magnetic moment force on each species is the vector sum of the forces generated by each component

$$\vec{F}_{\alpha m} = \vec{F}_{\alpha m}\left(B_y\right) + \vec{F}_{\alpha m}\left(B_z\right) \tag{20}$$

This generalization ensures that the model remains valid for reconnection geometries with a non-negligible guide field.

In summary, the modified two-fluid MHD equations presented above provide a unified theoretical foundation for describing magnetic reconnection. These revisions are systematically derived from a consistent kinetic picture, not ad hoc, and have simultaneously led to new interpretations of plasma thermal conductivity [21], anomalous transport in tokamak plasmas [19], and the magnetic reconnection rate. By incorporating the magnetic moment force as the correct gyro-averaged Lorentz force and by enforcing the semi-free electron constraint as a direct consequence of quasi-neutrality, the present formulation consistently bridges the gap between local microscopic kinetics and macroscopic reconnection dynamics. These modifications are therefore essential for capturing the full physics of fast reconnection, including the universal rate scaling and the bipolar electrostatic field structures, both of which are in quantitative agreement with observations in space and laboratory experiments.

3.5 Model applicability and limitations

The analytical model and the revised two-fluid equations presented above are derived under a specific set of physical assumptions. A clear delineation of these assumptions and their associated boundaries is essential for the correct interpretation and application of the present theory, and to prevent its misapplication to regimes where the underlying physics differs fundamentally.

The replacement of the Lorentz force by the magnetic moment force in Eq. (1) relies on the standard guiding-center approximation, which is valid when the magnetic field varies weakly over a gyroperiod and a gyroradius. The formal condition is given by $|r_{c\alpha}\nabla B/B| \ll 1$. This condition is generally satisfied in macroscopic space and astrophysical plasmas, such as the magnetotail and the solar wind, where the characteristic gradient scale lengths are much larger than the ion and electron Larmor radii.

The derivation of the closed-form reconnection rate in Eq. (13) is based explicitly on a two-dimensional, steady-state configuration. This framework is directly applicable to canonical reconnection geometries such as the magnetopause and the geomagnetic tail, where the quasi-steady reconnection is well-established.

The model, in its present form, is not applicable in two cases. One is the transient, explosive reconnection events (e.g., the impulsive phase of solar flares), where time-dependent effects and fast-growing instabilities dominate. The other is the system with a strong guide field that introduces significant three-dimensional variations. A rigorous generalization of the full rate expression to a 3-D geometry with a strong out-of-plane field requires a separate, more complex treatment and is beyond the scope of this work.

The core conceptual innovation of this work is the semi-free electron constraint expressed in Eq. (2), which eliminates ∇p_e as a macroscopic force. This constraint is a direct consequence of strict quasi-neutrality. This condition is robust in the vast majority of space and laboratory reconnection experiments. The fact that the derived bipolar electric field structure quantitatively matches satellite observations [2, 22] serves as a posteriori validation of this semi-free electron picture in these large-scale environments. However, it is not applicable to regimes where high-frequency electrostatic waves (e.g., Langmuir waves, ion acoustic waves) or kinetic instabilities prevail. In such cases, charge separation and electron inertia become essential and violate the local quasi-neutrality assumption underlying the semi-free electron constraint. Consequently, this picture should be regarded as a complementary framework for charge-neutral transport phenomena, rather than a universal alternative to high-frequency kinetic theory.

4. Conclusion

In this work, we have presented a new analytical model for two-dimensional magnetic reconnection that resolves the long-standing puzzle of the fast, universal reconnection rate of order 0.1. The model is built on two key insights: (i) the magnetic moment force is the correct kinetic-scale driver for the inflow; and (ii) the semi-free electron constraint eliminates the electron pressure gradient as a genuine macroscopic force. The derived reconnection rate is independent of system size, magnetic field, density, and resistivity, explaining the observed universality of the rate. For a thermal equilibrium hydrogen plasma, $R_{mr}\approx0.2$, in quantitative agreement with observations and simulations. The model also correctly predicts the bipolar normal electric field structure observed at the current sheet center.

Comparisons with the Sweet-Parker, Petschek, and Hall-MHD models show that our framework offers a more fundamental kinetic explanation, without invoking anomalous resistivity or slow shocks. The maximum reconnection rate is shown to be a thermodynamic property of the plasma, as determined by T_e/T_i and Z rather than a consequence of geometry.

Building on these results, we have proposed a consistent revision of the two-fluid MHD equations, eliminating ∇p_e and replacing the Lorentz force with the magnetic moment force. These revisions emerge naturally from the same unified kinetic picture that has simultaneously led to new interpretations of plasma thermal conductivity and anomalous transport in tokamak plasmas. This work provides a self-consistent, first-principles explanation for the fast reconnection rate and offers a solid foundation for future studies of cross-scale coupling in plasma physics.

References

[1] E. G. Zweibel, M. Yamada. Magnetic reconnection in astrophysical and laboratory plasmas. *Annu. Rev. Astron. Astrophys.*, **47**(2009)291-332.

[2] M. Yamada, R. Kulsrud, H. Ji. Magnetic reconnection. *Rev. Mod. Phys.*, **82**(2010)603-664.

[3] J. L. Burch, R. B. Torbert, T. D. Phan, L.-J. Chen, T. E. Moore, R. E. Ergun, J. P. Eastwood, D. J. Gershman, P. A. Cassak, M. R. Argall, S. Wang, M. Hesse, C. J. Pollock, B. L. Giles, R. Nakamura, B. H. Mauk, S. A. Fuselier, C. T. Russell, R. J. Strangeway, J. F. Drake, M. A. Shay, Y. V. Khotyaintsev, P.-A. Lindqvist, G. Marklund, F. D. Wilder, D. T. Young, K. Torkar, J. Goldstein, J. C. Dorelli, L. A. Avanov, M.

Oka, D. N. Baker, A. N. Jaynes, K. A. Goodrich, I. J. Cohen, D. L. Turner, J. F. Fennell, J. B. Blake, J. Clemmons, M. Goldman, D. Newman, S. M. Petrinec, K. J. Trattner, B. Lavraud, P. H. Reiff, W. Baumjohann, W. Magnes, M. Steller, W. Lewis, Y. Saito, V. Coffey, M. Chandler. Electron-scale measurements of magnetic reconnection in space. *Science*, **352**(2016)aaf2939(1-10).

[4] M. Hesse, P. A. Cassak. Magnetic reconnection in the space sciences: Past, present, and future. *J. Geophys. Res. Space Phys.*, **125**(2020)e2018JA025935.

[5] E. N. Parker. Sweet's mechanism for merging magnetic fields in conducting fluids. *J. Geophys. Res.*, **62**(4) (1957)509-520.

[6] P. A. Sweet. The neutral point theory of solar flares. In B. Lehnert, editor, *Electromagnetic Phenomena in Cosmical Physics*, Cambridge University Press, New York, 1958, pages 123-134.

[7] E. Priest and T. Forbes. *Magnetic Reconnection: MHD Theory and Applications*, Cambridge University Press, Cambridge, UK, 2000, pages 116-120.

[8] H. E. Petschek, Magnetic field annihilation. In *Proc. AAS-NASA Symp. Phys. Solar Flares*, NASA SP-50, 1964, pages 425-439.

[9] D. Biskamp, Magnetic reconnection via current sheets. *Phys. Fluids*, **29**(5) (1986)1520-1531.

[10] L. Malyshkin, T. Linde, R. M. Kulsrud. Magnetic reconnection with anomalous resistivity in two-and-a-half dimensions. I. quasistationary case, *Phys. Plasmas*, **12**(2005)102902(1-14).

[11]J. Birn, J. F. Drake, M. A. Shay, B. N. Rogers, R. E. Denton, M. Hesse, M.

Kuznetsova, Z. W. Ma, A. Bhattacharjee, A. Otto, P. L. Pritchett. Geospace Environmental Modeling (GEM) magnetic reconnection challenge. *J. Geophys. Res.*, **106**(A3) (2001)3715-3719.

[12] Y.-H. Liu, M. Hesse, F. Guo, W. Daughton, H. Li, P. A. Cassak, M. A. Shay. Why does steady-state magnetic reconnection have a maximum local rate of order 0.1? *Phys. Rev. Lett.*, **118**(2017)085101(1-6).

[13] M. A. Shay, J. F. Drake, B. N. Rogers, R. E. Denton. Alfvénic collisionless magnetic reconnection and the Hall term. *J. Geophys. Res.*, **106**(A3) (2001)3759-3772.

[14] Y.-H. Liu, P. Cassak, X. C. Li, M. Hesse, S.-C. Lin, K. Genestreti. First-principles theory of the rate of magnetic reconnection in magnetospheric and solar plasmas. *Commun. Phys.*, **5**(2022)97(1-9).

[15] P. A. Cassak, Y.-H. Liu, M. A. Shay. A review of the 0.1 reconnection rate problem. *J. Plasma Phys.*, **83**(5) (2017)715830501(1-17).

[16] Y. Kuramitsu, K. Sakai, T. Moritaka. Electron scale magnetic reconnections in laser produced plasmas. *Rev. Mod. Plasma Phys.*, **7**(2023)24(1-53).

[17] Y.H. Liu, M. Hesse, K. Genestreti, R. Nakamura, J. L. Burch, P. A. Cassak, N. Bessho, J. P. Eastwood, T. Phan, M. Swisdak, S. Toledo-Redondo, M. Hoshino, C. Norgren, H. Ji, and T. K. M. Nakamura. Ohm's Law, the reconnection rate, and energy conversion in collisionless magnetic reconnection. *Space Sci. Rev.*, **221**(2025)16(1-74).

[18] R. Nakamura, J. L. Burch, J. Birn, L.-J. Chen, D. B. Graham, F. Guo, K.-J. Hwang, H. Ji, Y. V. Khotyaintsev, Y.-H. Liu, M. Oka, D. Payne, M. I. Sitnov, M. Swisdak, S. Zenitani, J. F. Drake, S. A. Fuselier, K. J. Genestreti, D. J. Gershman, H. Hasegawa, M.

Hoshino, C. Norgren, M. A. Shay, J. R. Shuster, and J. E. Stawarz. Outstanding questions and future research on magnetic reconnection. *Space Sci. Rev.*, **221**(2025)17(1-22).

[19] Y.J. Huang, Magnetic Moment Force and Semi-Free Electrons: a Unified Analytical Theory for Anomalous Transport in Tokamak Plasmas, viXra:2512.0050.

[20] J. L. Xu, S. X. Jin, Plasma Physics, Atomic energy press, Beijing, 1981.

[21] Y.J. Huang, Analytical Model for the Thermal Conductivity of Fully Ionized Plasmas, viXra:2503.0090.

[22] J. R. Wygant, C. A. Cattell, R. Lysak, Y. Song,J. Dombeck, J. McFadden, F. S. Mozer, C. W. Carlson, G. Parks,E. A. Lucek, A. Balogh, M. Andre, H. Reme, M. Hesse, C. Mouikis Cluster observations of an intense normal component of the electric field at a thin reconnecting current sheet in the tail and its role in the shock-like acceleration of the ion fluid into the separatrix region. *J. Geophys. Res. Space Phys.* **110** (2005)A09206.

[23] F. S. Mozer, S.D. Bale, T. D. Phan, Evidence of Diffusion Regions at a Subsolar Magnetopause Crossing, *Phys. Rev. Lett.*, **89**(2002) 015002 (1-4).

[24] D. A. Uzdensky, R. M. Kulsrud, Two-dimensional numerical simulation of the resistive reconnection layer, *Phys. Plasmas*, **7**(2000)4018-4030.

[25] Alexander Piel, Plasma Physics: An introduction to laboratory, space, and fusion plasmas, 2nd edition, 2017, Springer International Publishing AG, Gewerbestrasse 11, 6330 Cham, Switzerland, pp.113-138.

[26] S. Eliezer, The Interaction of High-Power Lasers with Plasmas, 2002, Institute of

Physics Publishing, London, UK, pp.47-64.